Turkish Journal of Physics

http://journals.tubitak.gov.tr/physics/

Research Article

Turk J Phys
(2019) 43: 272 – 279
© TÜBİTAK
doi:10.3906/fiz-1812-26

Localizable entanglement of isotropic antiferromagnetic spin-1/2 chain

İzzet Paruğ DURU*, Şahin AKTAŞ
Department of Physics, Faculty of Arts and Sciences, Marmara University, İstanbul, Turkey

Received: 30.12.2018 • **Accepted/Published Online:** 03.05.2019 • **Final Version:** 12.06.2019

Abstract: The bounds of entanglement on antiferromagnetic (AF) isotropic Heisenberg spin-1/2 chain including dipole–dipole interaction (D) were investigated. The Quantum Monte Carlo method based on loop algorithm was employed to calculate the two-spin and single-spin expectation values mediating the lower and upper bounds. It was revealed that D and B_z (the applied magnetic field) were pivotal parameters in controlling either entanglement creation/extinction or entanglement enhancement/weakening. Rival regions indicated a revival phenomenon depending on the temperature for various strengths of D which also showed a nonmonotonic behavior under certain B_z identifying critical points. Even if thermal agitations break the stability of strong D entanglement, it remains invariable at very low temperatures.

Key words: Localizable entanglement, loop algorithm, Heisenberg model, dipole–dipole interaction

1. Introduction

Quantum entanglement, as a fascinating kind of quantum correlation, enables a strong "spooky" interdependence between the subparts of a system. It is an important tool on performing dense coding [1–3], teleportation [4], quantum computing, and information processes [5–7]. Also, it is an eligible tool to precisely understand the quantum phase transitions (QPTs), particularly in condensed matter physics. Heisenberg model is an appropriate candidate to study entanglement due to its literal and simplistic structure [8–10]. A wide range of studies have focused on both isotropic, anisotropic, AF (antiferromagnetic), and mixed Heisenberg systems with either absence or presence of external fields by neglecting dipole–dipole interactions [11–20]. Various entanglement measurement methods allow investigations in both bipartite and multipartite entanglement such as concurrence, entanglement witness, entanglement entropy, and localizable entanglement (LE) which are used to reveal the dependence of entanglement on certain physical quantities, e.g., anisotropy and magnetic field [11–21]. In spin systems, localizable entanglement ensures the maximum amount of bipartite entanglement via performing local measurement on the remaining part of multipartite system. Analytical and numerical solutions especially Quantum Monte Carlo simulations (QMCs) are intensely used to investigate the quantum correlations on aforementioned Heisenberg models in the lack of dipole–dipole interactions. Arnesen et al. [21] indicated a range of critical temperature values which cause vanishing of entanglement, however, increasing temperature actually enhanced the entanglement of spin pairs. Thermal entanglement measurements based on concurrence of isotropic XY model zero-field, provide maximized entanglement in ground state whereas strong external magnetic field was the main reason for extinction of entanglement at $T = 0$ [11]. As stated in [19], the second order QPT under zero-field and revival phenomena were observed for AF spin-1/2 chain in the lack of

*Correspondence: parugduru@gmail.com

dipole–dipole interaction. DaSilva found that entanglement increased with increasing exchange constant J of spin-1/2 particles located at adjacent sites of the lattice [20].

In this study, the effect of dipole–dipole interaction on LE was investigated, and the lower and upper bounds were determined in the case of AF isotropic Heisenberg spin-1/2 chain where exchange, Zeeman and dipole–dipole interactions were included to the Heisenberg Hamiltonian. Bounds of localizable entanglement were ascertained by QMC method based on loop algorithm. ALPS package [22] was used to simulate the spin-1/2 Heisenberg chain resulting in expectation values. Bounds were constructed with these simulated values via a simple python script. The long-ranged entangled pairs of spins (qubits) were traced to provide a distant information transfer.

2. Materials and methods

Heisenberg Hamiltonian of 1D spin-1/2 chain is described by Eq. (2.1), where J_x, $J_y J_z$ are exchange constants, B_z is the applied magnetic field, and $\hat{H}_D$ represents the dipole–dipole interaction. The first term is the exchange interaction and the second one denotes the Zeeman energy which originates from applied external field B_z. $\hat{H}_D$ is explicitly described in Eq. (2.2). Note that D is used to determine the strength of dipole–dipole interaction and r_{jk} is the distance between spin-1/2 particles. $\hat{S}_i^x$, $\hat{S}_i^y$ and $\hat{S}_i^z$ represent Pauli spin matrices.

$$\hat{H} = -\sum_{i=1}^{N} (J_x \hat{S}_i^x \hat{S}_{i+1}^x + J_y \hat{S}_i^y \hat{S}_{i+1}^y + J_z \hat{S}_i^z \hat{S}_{i+1}^z) - \frac{B_z}{2} \sum_{i=1}^{N} (\hat{S}_i^z + \hat{S}_{i+1}^z) + \hat{H}_D \tag{2.1}$$

$$\hat{H}_D = D \sum_{j=1}^{N} \sum_{k=1}^{N} \left[\frac{\vec{S}_j . \vec{S}_k}{r_{jk}^3} - 3 \frac{\left(\vec{S}_j . \vec{r}_{jk}\right)\left(\vec{S}_k . \vec{r}_{jk}\right)}{r_{jk}^5} \right] \tag{2.2}$$

All the possible states of the two spins are handled with density matrix, $\hat{\rho} = \frac{e^{-\beta \hat{H}}}{\sum e^{-\beta \hat{H}}}$ (thermal equilibrium) where $\beta = \frac{1}{k_B T}$ denotes the inverse temperature and k_B is the Boltzmann constant. The denominator of this fraction is called as partition function and describes the statistical properties including two-spin correlations of a system in thermal equilibrium. Figure 1 illustrates the 1D Heisenberg spin-1/2 chain at low (Figure 1a) and high (Figure 1b) temperatures, respectively, and spin pairs on which the entanglement measurement was performed are linked with curved-up lines.

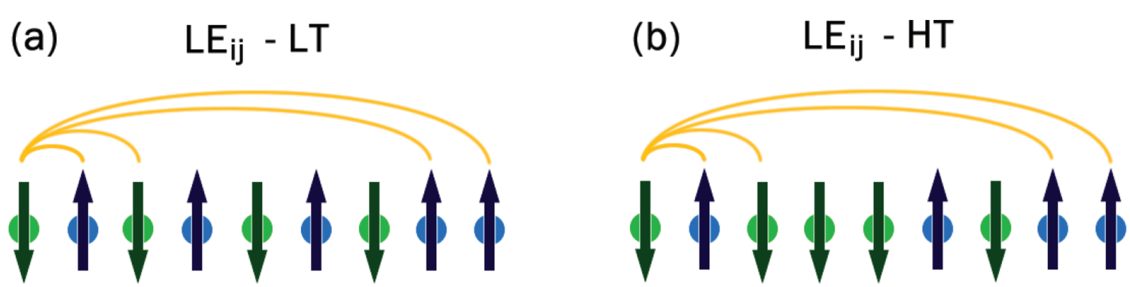

Figure 1. Illustration of 1D AF spin-1/2 chain at (a) low and (b) high temperatures.

LE provides an important way to determine the maximum amount of entanglement between the two parts of a system via performing local measurements on the rest part. Popp et al. [8] suggested measuring LE by declaring assistive notions as upper and lower bounds ($LE_{ij}^{lb} \leq LE_{ij} \leq LE_{ij}^{up}$). The lower bound ($LE_{ij}^{lb}$) is directly connected to the two-point correlation function $Q_{ij}^{\alpha\beta}(\psi)$ for a given pure state $|\psi\rangle$ of N qubits (Eq. (2.3)).

$$Q_{ij}^{\alpha\beta}\left(\psi\left|S_i^{\alpha}\otimes S_j^{\beta}\right|\psi\right)=\left\langle\psi\,|\,S_i^{\alpha}\otimes S_j^{\beta}\,|\,\psi\right\rangle-\langle\psi\,|\,S_i^{\alpha}\,|\,\psi\rangle\left\langle\psi\,|\,S_j^{\beta}\,|\,\psi\right\rangle \tag{2.3a}$$

$$LE_{ij}^{lb}= max(\left|Q_{ij}^{xx}\right|\left|Q_{ij}^{yy}\right|\left|Q_{ij}^{zz}\right|) \tag{2.3b}$$

Besides, upper bound (LE_{ij}^{ub}) is based on entanglement of assistance (EoF) and generally is formulated as in Eq. (2.4) [8,23,24].

$$LE_{ij}^{ub}=\frac{1}{2}\left(\sqrt{\left(1+\langle S_i^z S_j^z\rangle\right)^2-\left(\langle S_i^z\rangle+\langle S_i^z\rangle\right)^2}+\sqrt{\left(1-\langle S_i^z S_j^z\rangle+\langle S_j^z\rangle\right)^2-\left(\langle S_i^z\rangle-\langle S_j^z\rangle\right)^2}\right) \tag{2.4}$$

Simulation processes are performed by constructing a chain with $N = 40$ spin-1/2 particles resulting in expectation values, $[ERR : md : MbegChr = 0x2329, MendChr = 0x232A, nParams = 1]$ and $[ERR : md : MbegChr = 0x2329, MendChr = 0x232A, nParams = 1]$ ($\alpha = x, y, z$ and $\beta = z$), using a loop algorithm [25,26]-based simulator which was already included in the ALPS package [22]. Note that the spin chain corresponds to an infinite chain between 10–100 spins [18,19]. We deemed 2×10^7 steps suitable for the measurement process (correlations and thermodynamic quantities) and 2×10^6 steps for the thermalization process, respectively. QMC simulations are executed using 24 threads to mimic the chain with parallel processing for various D, kT, and B_z values, at a temperature scale $kT \in (0, 4]$.

3. Results and discussion

Exchange coupling constants, $J_\alpha\,(\alpha = x, y, z)$, were set as –1 for AF isotropic model. The bound values of nearest neighboring spins (qubits) were calculated under zero field for various D strengths at certain temperature values in terms of kT. At first sight, it can be clearly seen in Figure 2 that LE_{ij}^{lb} values monotonically increased via ascending D strengths while a decreasing behavior took place while increasing temperature as it can be naturally expected. Furthermore, LE_{ij}^{lb} values never vanished even at high temperatures. Note that only the two-site terms, that originated from the exchange and dipole–dipole interactions, were in charge. We deduced that LE_{ij}^{lb} did not lose unity with overlapping of all D strengths (except when $D = 0$) at present temperature scale (not shown here).

Thermal agitations led LE_{ij}^{lb} to diminish but LE_{ij}^{lb} did not completely vanish under zero field (Figure 2). According to Figure 3a, a similar behavior was also observed under applied field $B_z = 0.5$. The applied field caused a decrement of LE_{ij}^{lb} values but they were only increased for strengths $D \geq 1$ at very low temperatures. Moreover, nonmonotonic behavior was not observed yet under the zero field and $B_z = 0.5$. On the other hand, LE_{ij}^{ub} (Figure 3b) lost unity, except for $D = 0$, at very low temperatures as soon as the temperature reached approximately 0.05. At higher temperatures above 0.05, thermal agitations could not break the unity. However, it should be noticed that increasing the temperature causes an increment in LE up to $kT = 0.05$ introducing a ladder-like attitude. LE_{ij}^{ub} values tend to decrease by increasing the strength of dipolar energy

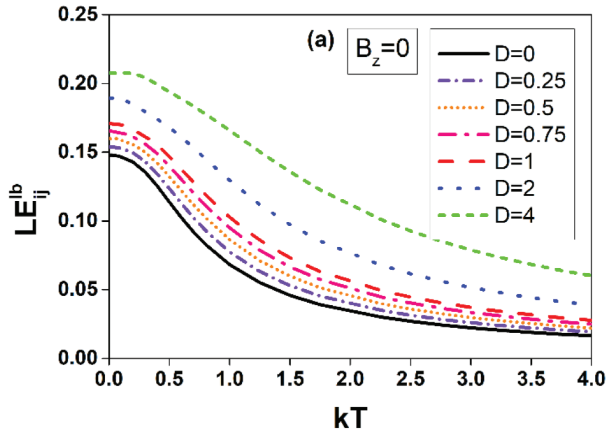

Figure 2. LE_{ij}^{lb} values of $D = 0$, 0.25, 0.5, 0.75, 1, 2, and 4 under zero-field ($B_z = 0$).

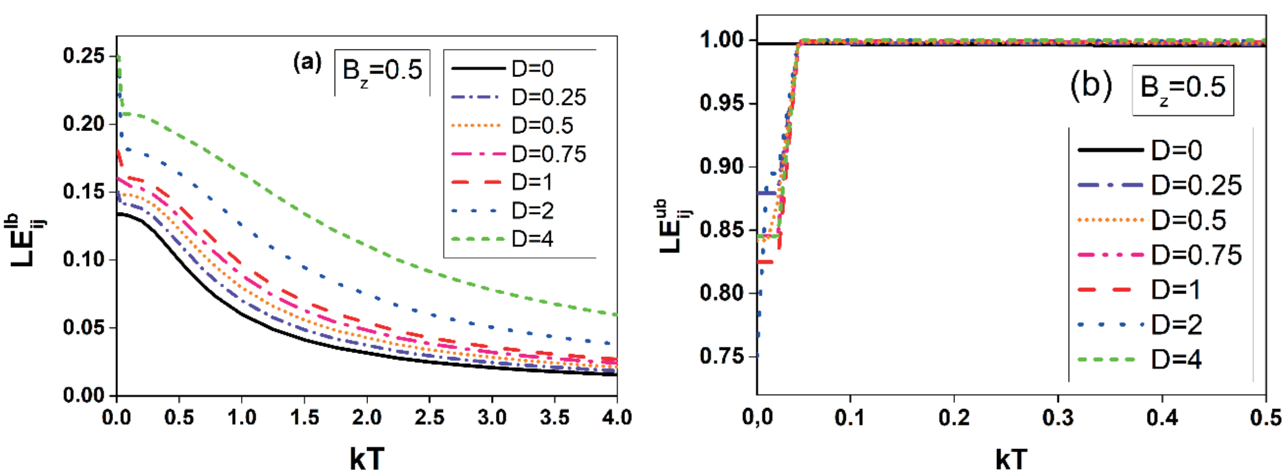

Figure 3. (a) LE_{ij}^{lb} (b) LE_{ij}^{ub} values of $D = 0$, 0.25, 0.5, 0.75, 1, 2, and 4 under $B_z = 0.5$.

up to $D = 2$ and increased by strengthening the dipolar interaction at very low temperatures. In short, a nonmonotonic behavior related to D is observed under $B_z = 0.5$ for $kT \to 0$.

Figure 4 shows $kT = 0.5$ denoting a critical point for $D = 0.75$ where LE_{ij}^{lb} vanishes and the entanglement gradually appeared at higher temperatures. It is also referred to as a nonmonotonic behavior of LE_{ij}^{ub} related to the temperature, namely, revival phenomena under $B_z = 2$ (Figure 4b). Furthermore, LE_{ij}^{lb} remained constant up to $kT \approx 0.2$ and exhibited a sharp decrement (SD) distinctly. Besides, LE_{ij}^{lb} (Figure 4a) illustrated a nonmonotonic behavior for $D = 0.5$ strength at $kT = 1.5$ indicating revival phenomena again. However, immediately after SD, LE_{ij}^{lb} increased up to $kT \approx 0.35$ and started to decrease with increasing temperature until $kT = 1.5$ is reached. In other words, $D = 0.5$ implicitly nominated two different critical points revealing revival phenomena under $B_z = 2$. Moreover, LE_{ij}^{lb} showed two different behaviors for $\leq D \leq 0.75$ and $0.75 \leq D \leq 4$, respectively, while the former ramp included an increasing trend in contrast to the latter ramp. In other words, $D = 0.75$ can be regarded as a critical point introducing a nonmonotonic attitude of LE_{ij}^{lb} related to D. According to Figure 4b, LE_{ij}^{ub} values increase via ascending D strengths monotonically for temperatures higher than $kT \geq 0.2$ even though they show a sharp rising, having distinct values at aforementioned temperature under $B_z = 2$.

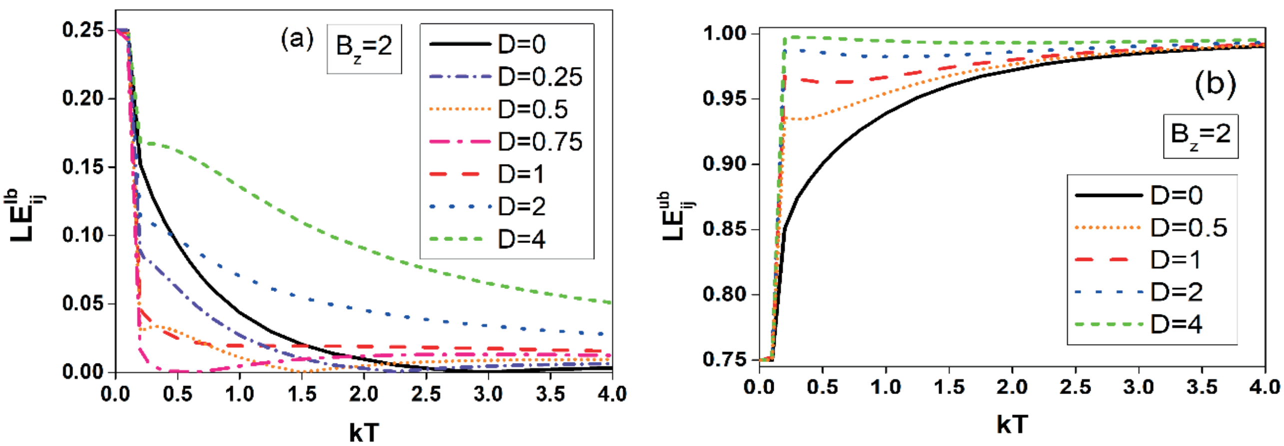

Figure 4. (a) LE_{ij}^{lb} (b) LE_{ij}^{ub} values of $D = 0$, 0.25, 0.5, 0.75, 1, 2, and 4 under $B_z = 2$.

LE_{ij}^{lb} values of corresponding D strengths, except when $D = 4$, are decreased monotonically depending on the increasing temperature and never vanished at present temperature scale (Figure 5a). Besides, LE_{ij}^{lb} is getting low via increasing D strengths. In fact, LE_{ij}^{lb} of $D = 4$ experienced a sudden drop at $kT \approx 0.25$ and extinction of entanglement occurred at $kT = 3$. It was concluded that LE_{ij}^{ub} values are increasingly proportional to both temperature and D strengths as illustrated in Figure 5b. One should remember that thermal agitations induce a strict resistance against two-site terms and the effect of external field but only if they disclose intrinsic phenomenological features such as odd-even effect and revival phenomena at critical points.

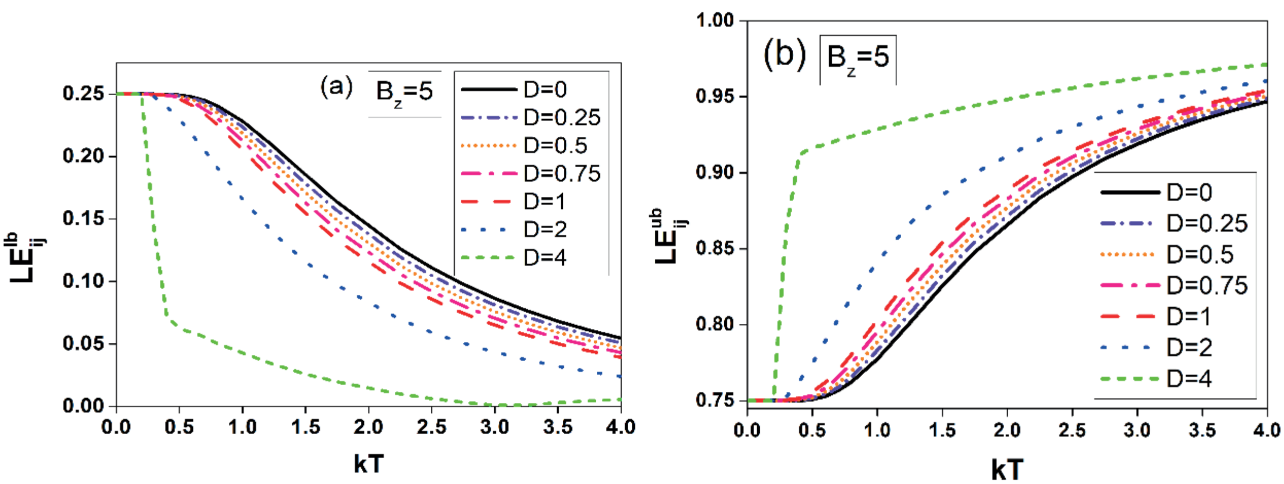

Figure 5. (a) LE_{ij}^{lb} (b) LE_{ij}^{ub} values of $D = 0$, 0.25, 0.5, 0.75, 1, 2, and 4 under $B_z = 5$.

Distant entanglement can enable a long ranged quantum information transfer, especially in spin chains under zero field. Hence, we focused on long-ranged bipartite entanglement among the nearest $n = 15$ neighboring spin pairs at very low ($kT = 0.05$) and low ($kT = 0.5$) temperatures under zero-field ($B_z = 0$). Figure 6 displays $LE_{i,i+n}^{lb}$ values for various D strengths under abovementioned physical conditions. According to Figure 6a, one can deduce that increasing D strength implicitly influences the lower bound and it remains unchanged up to $n = 15th$ nearest neighbor for $D = 2$ and $D = 4$ as well as at $kT= 0.05$. However, increasing the temperature causes an exponential attitude which results in the extinction of entanglement after $n = 10th$ neighbors for $D = 1$, $n = 7th$ for $D = 0$ except when $D = 4$, and $D = 2$ at $kT= 0.5$ (Figure 6b). We have also emphasized that entanglement never vanishes for $D = 4$ although increasing temperature starts to agitate the spin chain. Relatively higher temperatures, such as $kT= 3.5$, extremely shortened the distance of entangled spin pairs (short-ranged communication) because the exchange and dipole–dipole interactions loosed theirs domination on the system.

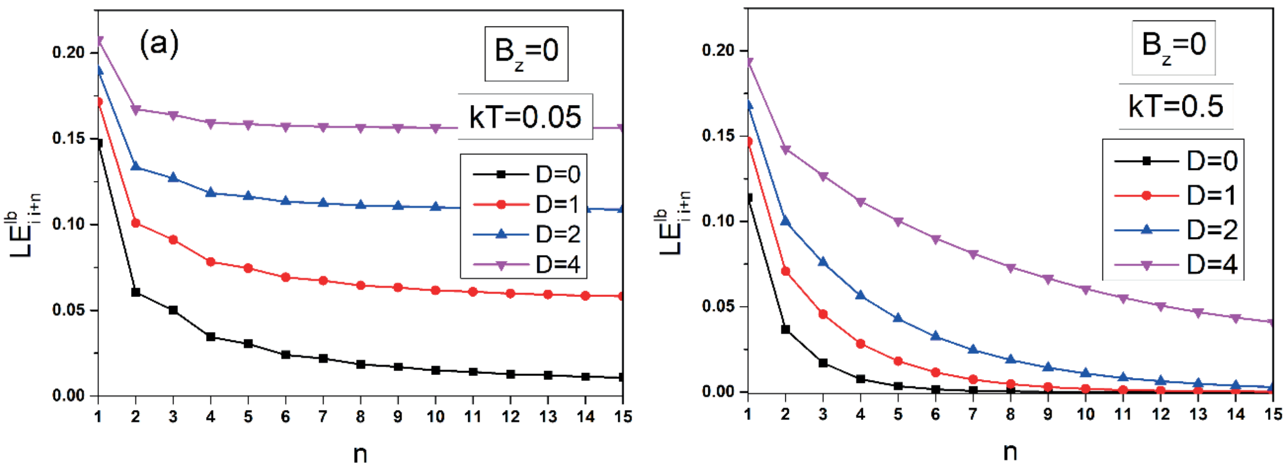

Figure 6. $LE^{lb}_{i,i+n}$ values of $n = 15$ nearest neighboring spins at temperature (a) $kT = 0.05$ (b) $kT = 0.5$.

Illuminating an inclusive picture, Figure 7 led us to evaluate $LE^{lb}_{i,i+n}$ depending on kT and distant neighboring pairs of spins simultaneously. Red regions verify the aforementioned sudden drop for specified D strengths under $B_z = 2$ as can be seen in the figure. Note that $D = 0.5$ and $D = 0.75$ strengths are inducing distinctive behaviors solely for the first nearest neighbors unless no influence takes effect along distant neighboring spin pairs. Existence of rival regions should be verified for the strengths of $D = 1$, $D = 2$, and $D = 4$ even when performing a cursory scan. $LE^{lb}_{i,i+2}$ $(n = 2)$ and $LE^{lb}_{i,i+4}$ $(n = 4)$ demonstrate a nonmonotonic behavior indicating rival regions at certain temperatures as $kT\approx 0.2$ (dark blue nearby yellowish) and likewise a rod shaped region for $n \geq 5$ (Figure 7a). According to Figure 7b, $D = 2$ induced a similar behavior for $n = 4$, $n = 6$, and very slight one for $n = 9$ distant spins at temperature $kT\approx 0.2$ where $LE^{lb}_{i,i+n}$ tends to vanish. However, rival regions are also formed as surrounding $kT = 1$ $(n = 4)$ and have a rod-like shape for $n \geq 6$. Moreover, strong dipole–dipole interaction ($D = 4$) possesses similar regions for odd numbered neighbors starting from $n = 3$ at various temperatures of kT even if $LE^{lb}_{i,i+n}$ values explicitly drop off involving first and second nearest neighbors at the present temperature scale (Figure 7c).

4. Conclusion

Entanglement measurements, especially bipartite entanglement, on many body systems can be successfully performed by QMC methods to reveal these "spooky" correlations between the nearest neighbors and distant pairs of particles since they possess a huge ability to be a resource for quantum information process. In this study, bounds of LE are determined to investigate the effect of dipole–dipole interaction on the evolution of entanglement in 1D Heisenberg spin-1/2 chain at temperature scale $kT\in (0, 4]$. The critical values are

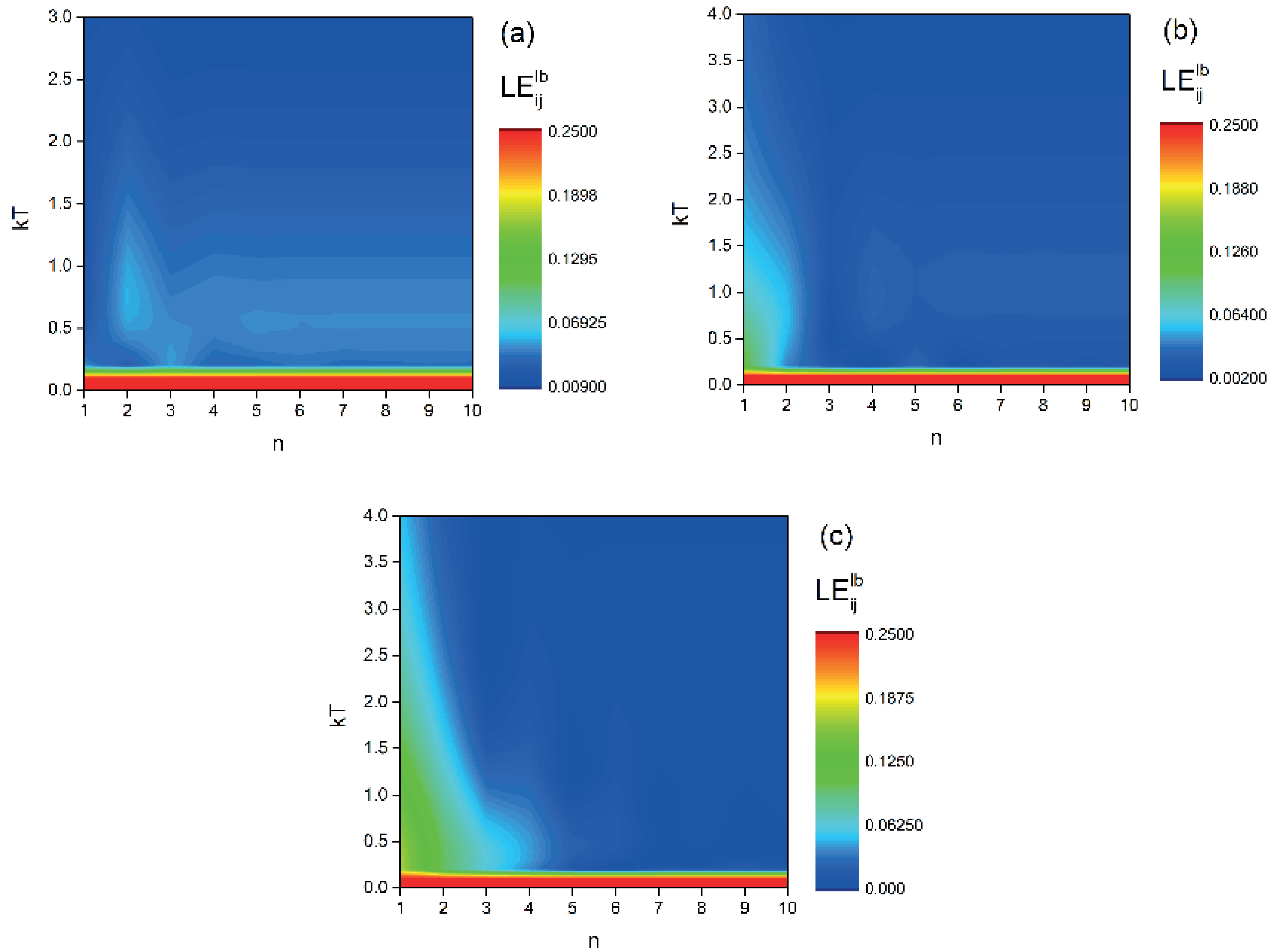

Figure 7. LE_{ij}^{lb} of $n = 10$ nearest neighboring spins under $B_z = 2$ with strengths (a) $D = 1$ (b) $D = 2$ (c) $D = 4$.

calculated and they indicate a nonmonotonic behavior which originated from the collaboration of kT, B_z, and, most particularly, strength of dipole–dipole interaction D. Revival phenomena are observed, but not limited to the nearest neighbors, along distant pairs of spins. Moreover, it is verified that a strong D enhances long-ranged entanglement at low temperatures under zero field, unless high temperatures reduce the distance. In the case of $kT \to 0$, a nonmonotonic behavior related to D is observed under $B_z = 0.5$. We emphasize that undominated systems tend to generate a nonmonotonic behavior even though relatively strong interactions provide a substantial regulation.

Acknowledgments

The authors would like to thank İlhan YAVUZ, Arife Saba KARAKAŞ, and Caner DEĞER for helpful comments on discussion of processed data. We also appreciate the valuable support of Lütfi ARDA and Ersin ÖZUĞURLU during the redaction of this paper. Simulations were performed in the Simulation and Modelling Research Laboratory (Simulab) at the Department of Physics, Marmara University.

References

[1] Bose, S., Plenio, M.B., Vedral, V. *Journal of Modern Optics.* **2000**, *47*, 291-310.

[2] Barenco, A.; Ekert, A. K. *Journal of Modern Optics.* **2007**, *42*, 1253-1259.

[3] Das, T.; Prabhu, R.; Sen(De), A.; Sen, U. *Phys. Rev. A.* **2015**, *92*, 052330.

[4] Nielsen, M. A.; Chuang, I. L. *Quantum Computation and Quantum Information*, First ed.; Cambridge University Press: Cambridge, UK, 2000.

[5] Dieks, D. *Phys. Lett. A.* **1982**, *92*, 271-272.

[6] Beige, A.; Braun, D.; Tregenna, B.; Knight, P. L. *Phys. Rev. Lett.* **2000**, *85*, 1762-1765.

[7] Field, B.; Simula, T. *Quantum Science and Technology*, **2018**, *3*, 59.

[8] Verstraete, F.; Popp, M.; Cirac,J.I. *Phys. Rev. Lett.***2004**, *92*, 027901.

[9] Popp, M.; Verstraete, F.; Martin-Delgado, M. A.; Cirac, J.I. *Phys. Rev. A.* **2005**, *71*, 042306.

[10] Jin, B-Q.; Korepin, V.E. *Phys. Rev. A.* **2004**, *69*, 062314.

[11] Wang, X. G. *Phys. Rev. A.* **2001**, *64*, 012313.

[12] Kamta, G. I.; Starace, A. F. *Phys. Rev. Lett.* **2002**, *88*, 107901.

[13] Syljuäsen, O. F. *Phys. Rev. A.* **2003**, *68*, 060301.

[14] Rigolin, G. *Int. J. Quantum Inf.* **2004**, *2*, 393-405.

[15] Canosa, N.; Rossignoli, R. *Phys. Rev. A.* **2006**, *73*, 022347.

[16] Jiang, C-L.; Fang, M-F.; Hu, Y-H. *Int. J. Theor. Phys.* **2009**, *48*, 1672-1677.

[17] Deng, D. L.; Gu, S. J.; Chen, J. L. *Annals of Physics.***2010**, *325*, 367-372.

[18] Androvitsaneas, P.; Paspalakis, E.; Terzis, A. F.*Annals of Physics*, **2012**, *327,* 212-223.

[19] Androvitsaneas, P.; Fytas, N.G.; Paspalakis, E.; Terzis, A. F. *Philosophical Magazine*, **2012**, *92,* 4649-4656.

[20] da Silva, S .L .L. *Quantum Stud.: Math. Found.* **2017**, 40509, 1-8.

[21] Arnesen, M. C.; Bose, S.; Vedral, V. *Phys. Rev. Lett.* **2001**, *87*, 017901.

[22] Bauer, B.; Carr, L. D.; Evertz, H. G.; Feiguin, A.; Freire, J.; Fuchs, S.; Gamper, L; Gukelberger, J.; Gull, E.; Guertler, S.; et al. *Journal of Statistical Mechanics: Theory and Experiment*, **2011**, P05001.

[23] DiVincenzo D. P.; Fuchs C. A.; Mabuchi H.; Smolin J. A.; Thapliyal A.; Uhlmann A. *Entanglement of Assistance.* In: Williams C.P. (eds) *Quantum Computing and Quantum Communications.* QCQC 1998. Lecture Notes in Computer Science, vol. 1509. Springer: Berlin, Heidelberg, Germany,1999.

[24] Laustsen, T., Verstraete, F., Enk, S. J. *Quantum Inf. Comput.* **2003**, *3*, 64-83.

[25] Evertz, H. G.;Lana, G.; Marcu, M. *Physical Review Letters*, **1993**, *70*, 875.

[26] Swendsen R. H.; Wang, J. S.*Physical Review Letters*, **1987**, *58,86.*